



LSU Health
NEW ORLEANS
School of Medicine

Ethanol dysregulates chondrocyte differentiation via different sources of reactive oxygen species in chondrocyte ATDC5 cells

Jonathan Lewis¹, James Watt² and Martin Ronis²

¹University of New Orleans ²Department of Pharmacology, LSU Health Sciences Center

Introduction

Understanding chondrocyte differentiation in the presence of oxidative stress is one key to unlocking the mechanism by which alcohol contributes to low bone density and osteoporosis. During differentiation, chondrocytes undergo phases of proliferation, hypertrophy and apoptosis accompanied by stage-specific gene expression, NADPH oxidases (NOX) enzymes, in particular NOX2 and NOX4-generated reactive oxygen species (ROS) have been found to be vital in chondrocyte differentiation. In contrast, ethanol ETOH has been shown to dysregulate bone turnover via NOX2 and NOX4 in osteoblasts¹⁻³ and suppress osteoblast differentiation in vivo via mitochondrial ROS. Additionally, it has been found that alcohol dysregulates the growth plate leading to an observed decrease of long bones in vivo. This effect is reversed through co-ingestion of antioxidant N-acetyl cysteine (NAC).⁴ The hypothesis of these studies is that alcohol will dysregulate chondrocyte differentiation but the correct dose and type of antioxidant will mitigate that effect.

Background

- Chondrogenesis is the complex process that leads to the establishment of cartilage and bone formation. Chondrocytes produce and maintain the growth plate of long bones.
- ATDC5 cells are an experimental model used to study chondrocyte differentiation.
- NOX 2, NOX 4 and mitochondria are potential sources of ROS in cells exposed to ethanol.
- Use of NOX specific and mitochondrial-targeting inhibitors and antioxidants can help isolate and identify sources of ROS
- EIOH can induce oxidative stress via each of these mechanisms

Methods

• ATDC5 culture: ATDC5 cells were plated at 1,000 cells/ml in 6-well plates in DMEM + 10% fetal bovine serum (FBS) for 24 hours. Cells were then treated with 0, 1, 10, 100, or 500 μM EIOH for 72 hours. Media were harvested and analyzed for ROS levels. Cell viability was determined using MTT assay.

• Gene Expression: Total RNA was extracted from ATDC5 cells treated with 1, 10, 100, or 500 μM EIOH for 72 hours. RNA was quantified and stored at -80°C until use.

• Chondrocyte Differentiation: ATDC5 cells were plated in 24-well plates in DMEM + 10% FBS for 24 hours. Cells were then treated with 0, 1, 10, 100, or 500 μM EIOH for 72 hours. Media were harvested and analyzed for ROS levels. Cell viability was determined using MTT assay.

Results

Figure 1. Alcian Blue stain for cartilage deposition in vitro in response to ETOH and antioxidant co-treatments

Figure 2. Alcian Blue Quantification

Figure 3. Alizarin Red stain for mineralization

Left: Alizarin Red and Alcian Blue staining from a previous study exhibited a negative correlation between EIOH concentration and in vitro cartilage formation while showing an increase in mineralization. As mineralization happens later in the differentiation of a chondrocyte, this data suggests a dysregulation of normal cartilage formation and chondrocyte mineralization by EIOH.

Gene Expression

Left: qPCR gene expression data from Day 12 of a previous study also showed a marked decrease with EIOH in the expression of Col2a1 and Acan. These findings prompted a time course study to determine whether EIOH produced an overall decrease in gene expression or a shift in peak gene expression at a different time point

Figure 4. Time course of gene expression in ATDC5 cells in response to ETOH/antioxidant co-treatment

Conclusion

- EIOH suppresses in vitro cartilage formation while increasing mineralization, suggesting a dysregulation of chondrocyte differentiation.
- Antioxidants did not seem to mitigate EIOH's dysregulation of cartilage formation, suggesting a role for endogenous ROS in cartilage formation.
- MitoQ and MitO TEMPO appear to block EIOH effects on mineralization. However, these effects and NAC appears to exacerbate EIOH effects.
- MitoQ's marked effect on to block EIOH effects on mineralization, the NOX inhibitor has no effects on chondrocytes. MitoQ's independent suppression of gene expression (Col2a1, Col10a1 and Acan) suggests that mitochondrial ROS plays a role in cartilage formation.
- Major differences between 10mM and 25mM EIOH-treated cells for Col2a1, Acan and Runx2 at Day 14 suggest that EIOH affects gene expression at later stages. More studies involving later stage gene expression of chondrocytes could shed more light on EIOH's ROS-independent suppression of genes related to cartilage formation.

• This research project was supported by grant # 1659752 through the National Science Foundation (NSF), Research Experiences for Undergraduates (REU) Program and NIAAA R37 AA018282 (M.R.)

Purification and Functional Analysis of Monoclonal Antibodies Protection Against *C. auris* Invasive Infections

Claudia Rodriguez, Abby Adams, Jonothan Colon, Karen Eberle, Dr. Hong Xin
Department of Microbiology, Immunology, and Parasitology LSUHSC New Orleans, LA



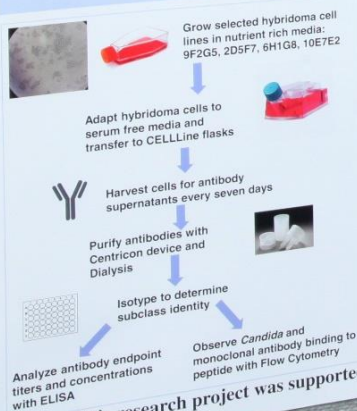
Introduction

Disseminated candidiasis is a life-threatening nosocomial infection, and is a leading cause of bloodstream infections affecting immunocompromised patients in the United States. Despite the advancements of antifungal therapies, the mortality rate remains unacceptably high. Due to its high mortality rate and burden on the healthcare system, novel approaches are needed to improve antifungal therapy. Among medically important *Candida* species, *C. auris* is a lethal fungus and has been identified over 700 cases in the United States as of July 2019. CDC refers to *C. auris* as a superbug because of its high mortality rate (30-60%), and it is multidrug resistant. This type of multidrug resistance has not been observed before in other species of *Candida*.

Preliminary data: Xin lab has identified and isolated a panel of monoclonal antibodies (mAbs) specific for *Candida* cell surface peptides, and the mAbs provide protection in mice against disseminated candidiasis caused by medically important *Candida* species, including *C. auris*.

Goals: The goal of this study was to produce protective mAbs by cell culturing hybridoma cells, adapt cells to CELLline flasks, and purify mAbs by using a Centricion device. Finally, ELISA, fluorescence staining and Flow cytometric analysis were performed to validate the binding of each mAb to specific *Candida* cell wall peptides.

Methods



Immunoassay Methods

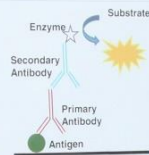


Fig. 1: ELISA was used to detect titers of purified mAb. EIA plates were coated with *Candida* cell wall peptides Fba, Met 6, GPV-P3, PgK1. Purified mAb were used as the primary antibody at varying dilutions. The secondary antibody was goat anti-mouse IgG-HRP. A similar method was used to determine mAb subclass identity.

Results

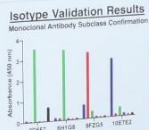


Fig 2: mAb subclass identity was verified for 2DSF7, 6H1G8, 9FZG5, 10E7E2 cell lines.

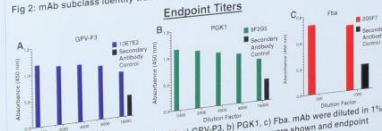


Figure 3: ELISA plates were coated with a) GPV-P3, b) PgK1, c) Fba. mAb were diluted in 1% bovine serum albumin (BSA) blocking buffer. Dose responses were shown and endpoint titers were recorded.

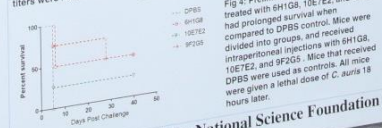


Fig 4: Preliminary data shows that mice treated with 6H1G8, 10E7E2, and 9FZG5 had prolonged survival when compared to 9FZG5 control. Mice were divided into groups, and received intraperitoneal injections with 6H1G8, 10E7E2, and 9FZG5. Mice that received 10E7E2, and 9FZG5 were used as controls. All mice were given a lethal dose of *C. auris* 18 hours later.

Flow Cytometry and Fluorescent Staining

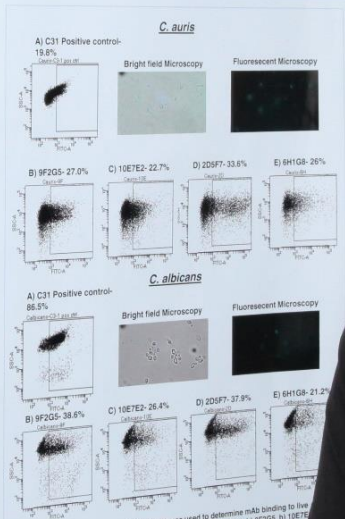


Fig 5: Flow cytometry and fluorescent staining was used to determine mAb binding to live *C. auris* and *C. albicans* yeast cells. The figure shows a) C31 (positive control), b) 9FZG5, c) 10E7E2, d) 2DSF7, and e) 6H1G8 mAb binding to *C. auris* (top panel) and *C. albicans* (bottom panel). Positive control observed under bright field and fluorescent microscopes.

Conclusions

- Immunassay results show evidence of high functional titers for 10E7E2 and 9FZG5 mAbs against *C. auris* and *C. albicans* yeast cells.
- We observed protection against disseminated infections through Flow cytometry, which provide protection against live *Candida* cells through Flow cytometry, of disseminated candidiasis.
- We observed antibody binding to live *Candida* cells through Flow cytometry, which provide protection against live *Candida* cells through Flow cytometry.
- Monoclonal antibody based therapy may hold the hope for treating *C. auris* disseminated infections in humans.

This research project was supported by grant # 1659752 through the National Science Foundation (NSF), Research Experiences for Undergraduates (REU) Program

Retinal Sensitivity in Hormonally Modulated *Hyla cinerea* Using Electrophysiological Techniques



¹Ashley Santana, ^{1,2}Whitney Walkowski M.S., ^{1,2}Hamilton Farris PhD

¹Neuroscience Center of Excellence, ²Department of Cell Biology and Anatomy, LSU Health, New Orleans, LA

Introduction

Hormones affect the performance of organs and tissues within the nervous system. The peripheral nervous system and its exposure of sensory receptors are the largest beneficiary from hormone modulation¹. However, little is known of how endocrine mechanisms modulate visual signals and the performance of the retinal layer. Epidemiological studies have shown that there is a correlation between ocular diseases and a decline in sex steroids in the retina's sensory layer². This project quantifies retinal function in the gravid, green tree frog *Hyla cinerea* to evaluate the effect of hormone modulation in visual systems. Reproductive states are hypothesized to increase retinal sensitivity, and have an effect on the performance of bipolar cells in the inner nuclear layer (INL) of the retina. Electroretinograms (ERGs) are the primary method for recording neural responses in the eye, and are used in this study to evaluate cellular activity between endocrine state and peripheral sensory function. Understanding the relationship between endocrine state and peripheral sensory function can potentially identify optimal biological conditions for retinal health.

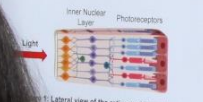


Figure 1: Lateral view of the retina and its nuclear layers.

Reproductive (endocrine) state affect Inner Nuclear Layer Response to light?

Scotopic ERGs

Animals were dark adapted in a light proof chamber. To immobilize the frog during the procedure, we used a light anesthetic. Responses were recorded from scotopic light flashes at 450nm, 550nm, 650nm, 650nm, 700nm, and 750nm. The amplitude of the B wave response for individual wavelengths based on the V Log(I) curves.

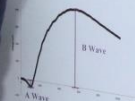


Figure 3: Graphical representation of an ERG response. The A wave represents the hyperpolarization of photoreceptors in the outer nuclear layer of the retina. The B wave is bipolar cell depolarization in the inner nuclear layer.

Results: Relative Spectral Sensitivity

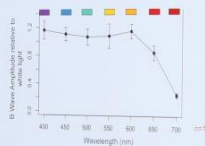


Figure 4: Average B wave amplitude for all experimental groups during isointensity (2.157 cds/m², 0.33 log cds/m²) stimulation at different wavelengths of light. F6.74±9.76; P<0.001

- Bipolar cell activity at longer wavelengths is relatively less in comparison to shorter wavelengths.
- Analysis of relative spectral sensitivity provides a broad overview of visual limitations, without considering photoreceptor saturation.

Results: V Log(I) Response Curves

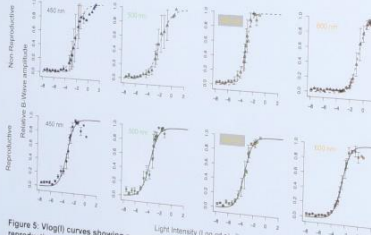


Figure 5: V Log(I) curves showing mean ERG responses for female non-reproductive and reproductive groups. Each point represents the mean relative B wave amplitude at each light intensity. Reproductive threshold is shifted left.

Discussion and Future Experimentation on Endocrine Modulation

Assay precise endocrine state. A and B are non reproductive and reproductive ovaries, respectively.



Identify endocrine targets in photoreceptor and INL that could mediate modulation of responses. Image shows unstimulated estradiol receptor in the INL. GFP, normally shown as GFP6.

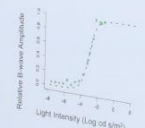


Figure 6: V Log(I) curve showing relative B wave amplitude at each light intensity for an hCG injected female. Compare to figure 5.

Discussion and Future Experimentation on Endocrine Modulation

- Relative spectral sensitivity data reveal the variation between non-reproductive and hormonally modulated retinal response.
- Retinal thresholds for individual wavelengths were calculated from ERGs following protocol 2. Hormonally modulated *Hyla cinerea* display a lower retinal threshold compared to non-reproductive groups.
- Bipolar cell response is emphasized in ERG traces. Further investigation into direct hormonal activity on Bipolar cells is needed to fully understand the underlying mechanisms mediating this effect.
- Clinical Significance: This modulation may enable a therapeutic tool to increase sensitivity in damaged retina.

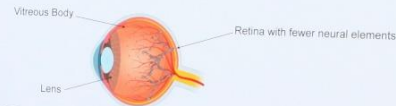


Figure 7: Eye with retinitis pigmentosa. Gray regions mark deterioration of the retina and vascular physiology. Individuals with this condition experience night blindness and progressive loss of the visual field.

Future Work

- Enzyme Linked Immunosorbent Assays will be used to verify hormone concentrations within the blood.
- Opsin sequencing will be conducted via Fluorescence in-situ hybridization to investigate location and advanced function in the retina.
- Computation of optimal retinal function and correlating reproductive hormone concentration has potential clinical applications for treating degenerative retinal diseases.

Acknowledgements

Preliminary data and images were collected with the assistance of doctoral candidate Whitney Walkowski and principal investigator Dr. Hamilton Farris. A large thank you to the National Science Foundation for funding the 2019 Research Experiences for Undergraduates Program at Louisiana State University Health Sciences Center.



References

- Klein, B. E., Klein, R., & Lee, K. E. (2000). Reproductive exposures, incident age-related cataracts, and age-related maculopathy in women. *The Beaver Dam Eye Study* 11. Reprints not available. *American Journal of Ophthalmology*, 130(3), 322-326. doi:10.1016/S0002-9394(00)00474-8
- Nazzi, R., Scalabrini, S., Becco, A., & Panzica, G. (2018). Gonadal Hormones and Retinal Disorders: A Review. *Frontiers in Endocrinology*, 9. doi:10.3389/fendo.2018.00066
- Klein BE, Klein R, Lee KE. Reproductive exposures, incident age-related cataracts, and age-related maculopathy in women: the Beaver Dam Eye study. *Am J Ophthalmol* (2000) 130(3):322-8. doi:10.1016/S0002-9394(00)00474-8
- Schemm M, Krafsnik R, Glaeser L, Kuntzer T, Bogouslavsky J, Barakat-Walter I. Thyroid hormone reduces the loss of axotomized sensory neurons in dorsal root ganglia after sciatic nerve transection in adult rat. *Exp Neurol*. 2003;184:225-236

This research project was supported by grant # 1659752 through the National Science Foundation (NSF), Research Experiences for Undergraduates (REU) Program

The Protein S LG1+2 Domain Contributes Significantly to Inhibition of Factor IX_a

Amber Sylvain, Sabyasachi Chatterjee, PhD, and Rinku Majumder, PhD
LSU Health Science Center.

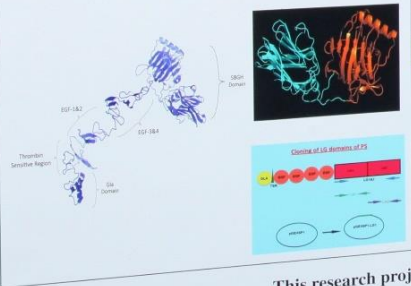


Introduction

Protein S (PS) is a vitamin K-dependent anticoagulant. PS deficiency may have severe—even deadly—outcomes, such as deep vein thrombosis, arterial thrombosis (stroke, heart attack), and pulmonary embolism. We have demonstrated a direct inhibition of FIXa by PS independent of Protein C, in the absence and presence of FVIIIa. However, the binding sites for FIXa within PS have not been identified, such identification is a necessary first step to enlisting PS in the prevention of life-threatening thrombosis. Thus, we used an *in silico* docking approach with the three dimensional structure of Sex Hormone Binding (SHBG) domain(s) of PS that predicted the involvement of SHBG domain to mediate FIXa binding. The SHBG is composed of mainly two laminin (LG)-type domains, LG1 and LG2. Anisotropy of active site-labeled FIXa (DEGR-IXa) in the presence of phosphatidylserine/phosphatidylcholine vesicles and increasing concentrations of LG1+2 constructs revealed a binding K_D of 50 nM, which was comparable to the binding K_D of intact PS to FIXa ($K_D \sim 40$ nM). We used Circular dichroism spectroscopy (CD), isothermal titration calorimetry (ITC), as well as *ex-vivo* plasma assays to identify the structural and functional interactions between LG domains of PS and factor IXa. CD spectroscopy identified the conformational changes, and ITC identified the association constant (K_a), binding stoichiometry (n), and thermodynamic parameters (ΔG , ΔS and ΔH) when the LG domains bind to FIXa. Furthermore, we used the physiologically relevant Thrombin Generation Assay (TGA) to identify whether LG domains could reduce peak thrombin formed in PS-deficient plasma. Finally, we determined aPTT clotting times of PS deficient plasma in the presence of LG1, LG2 and LG1+2 domains. Furthermore, we determined that the LG1+2 domain, and LG1 or LG2 domain could mimic the effect of intact PS in inhibiting FIXa.

Objectives

Which of the two Laminin G like domains—if not both—are responsible for binding to and inhibiting coagulation FIXa?



Circular Dichroism (CD)

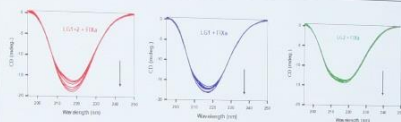


Figure 1 The change on CD spectra of LG1+2, LG1, and LG2 (2.5 μM) domain of PS with binding with 0.0, 25.0, 5.0, 75.1, and 1.25 μM of FIX_a. The conformational changes are 15.49%, 9.04%, and 3.02 % for LG1+2, LG1 and LG2 respectively.

Isothermal Titration Calorimetry (ITC)

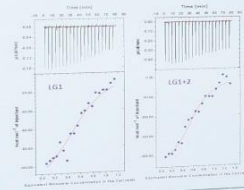


Figure 2 ITC of the interaction of LG1 and LG1+2 domains of PS with FIXa. The top panel shows raw data of sequential concentrations of FIXa into LG1 and LG1+2 domains. The bottom panel represents the integrated heat result of the titrations.

ITC Data

	LG1	LG1+2
n	0.649	0.6
K_D	$5.16 \times 10^6 M^{-1}$	$1.2 \times 10^6 M^{-1}$
ΔG	-8.9 kcal/mol	-9.4 kcal/mol
ΔH	-73.25 kcal/mol	-239 kcal/mol
$T\Delta S$	-64.16 kcal/mol	-216.2 kcal/mol

Table 1. Parameters determined by ITC between LG1 and LG1+2 constructs of PS with FIXa.

ex-vivo Plasma Assays Data

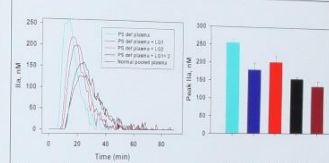


Figure 3. Thrombin generation assays were performed with PS deficient plasma supplemented without or with different LG domain constructs. The reactions were initiated with low TF (0.4 pm) to selectively generate thrombin in the intrinsic pathway. The thrombin generation was also performed with normal pooled plasma.

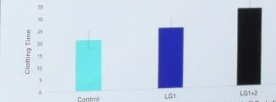


Figure 4. Clotting Assay showing the clotting times of PS deficient plasma as a control and in the presence of LG1 and LG1+2 (3 μM) domains.

Conclusion

The CD spectra showed significant conformational changes in LG1 and LG1+2 domains upon binding with FIXa. However, the change in conformation was maximum with LG1+2 domain. ITC data showed similar results, demonstrating that the interaction between PS and FIXa is exothermic, driven by a negative enthalpy change. Concluded from the negative Gibbs free energy value, we concluded from the negative Gibbs free energy value, the association constant (K_a) (Table 1), that the interaction between PS and FIXa was comparatively more feasible than that of LG1 with FIXa. The stoichiometry of bindings of both LG1+2 and LG1 with FIXa was comparatively more feasible than that of LG1 with FIXa. The binding of LG1+2 with FIXa was more stronger than with LG1. The TGA and TGA supported the results from the clotting assay showed increased clotting time with the addition of LG1+2, and TGA supported the results from the clotting assay showed increased clotting time with the addition of LG1+2, and TGA supported the results from the clotting assay showed increased clotting time with the addition of LG1+2. On the basis of these results, we conclude that the LG1+2 domain of PS is binding to and inhibit FIXa.

This research project was supported by grant # 1659752 through the National Science Foundation (NSF), Research Experiences for Undergraduates (REU) Program



Health
NEW ORLEANS
Medicine

Neuroadaptations in
Animal Model of Complex
Alcoholism

Amy P. Urbina, Jessica A. Cucinello, K...
Department of Physiology, LSU
Tulane

Introduction

Regional Pain Syndrome (CRPS) is a
condition that occurs following injury
to a limb
It disproportionately affects women.

Many symptoms
Anxiety, depression, neuropathy,



Alterations in Estrogen

Timeline of the experiment, (B) Visual
analysis test, (C) Additive effects of cast
alcohol 3 days after cast removal using the
PER (n=4 per group).

Analysis revealed that alcohol did
alter the level of Estrogen 11β, (B) expression
of Estrogen 11β, (C) expression of
PER (n=4 per group).

supported by grant # 1659752
Research Experiences for Undergraduates

42

Contributes Significantly to Factor IX_a, Ph.D., and Rinku Majumder, Ph.D. Science Center.



ex-vivo Plasma Assays Data

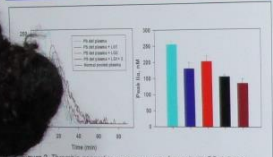
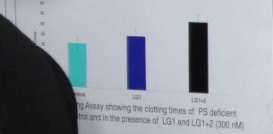


Figure 3. Thrombin generation assays were performed with PS deficient plasma supplemented without or with different LG1 domain constructs. The reactions were initiated with low TP (0.4 μM) to selectively generate thrombin in the intrinsic pathway. The thrombin generation was also performed with normal pooled plasma.



Conclusion

we observed significant conformational changes with LG1 binding in our model system. This was demonstrated by the interaction between FXIII and FXIIIa, driven by a negative entropy and enthalpy. The negative Gibbs free energy values (ΔG) and the findings were more feasible than that of LG1 with FXIIIa. Through the analysis of both LG1+2 and LG1 with FXIIIa, though the binding of FXIIIa was more stronger than with LG1 (Table 1), the increased clotting time with the addition of LG1+2 domain reduced the peak thrombin to the highest. Our results conclude that the LG1+2 domain of PS could be a potential target for FXIIIa.

43



Neuroadaptations in Estrogen Signaling in an Animal Model of Complex Regional Pain Syndrome & Alcoholic Neuropathy

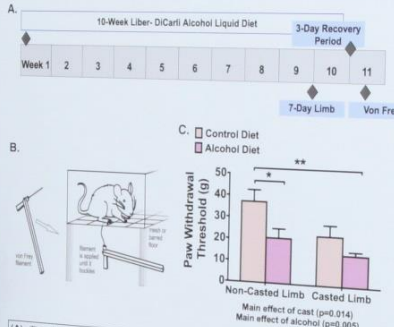


Amy P. Urbina, Jessica A. Cucinello, Kimberly N. Edwards, Liz Simon, Scott Edwards
Department of Physiology, LSU Health Sciences Center- New Orleans
Tulane University

Introduction

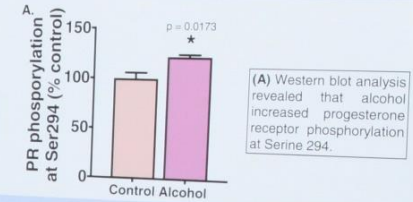
Complex Regional Pain Syndrome (CRPS) is a chronic pain condition that occurs following injury to a limb.

Behavioral Analysis



(A) Timeline of the experiment. (B) Visual Representation of the Von Frey hyperalgesia test. (C) Additive effects of cast immobilization and chronic alcohol on hyperalgesia 3 days after cast removal using the Von Frey test (n=8-10 per group). Main effect of alcohol (p<0.005)

Alterations in Progesterone Signaling



(A) Western blot analysis revealed that alcohol increased progesterone receptor phosphorylation at Serine 294.

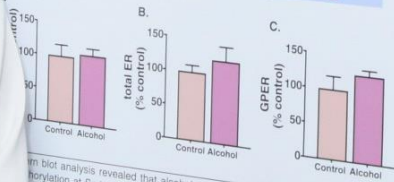
Conclusions

- Behavioral data demonstrate that chronic alcohol intake increased pain sensitivity in our model of CRPS.
- Although the difference in the expression of several estrogen receptors was not statistically significant, there was a general trend for alcohol to increase the expression of total ER and GPER.
- An alcohol liquid diet led to an increase in progesterone receptor phosphorylation at Serine 294 in the cingulate cortex.

Future Directions

- Future analysis will investigate other pain-related brain regions, including the prefrontal cortex and central amygdala.
- Because pain and motor information travel contralateral, future research will investigate if neuroadaptations to alcohol and CRPS are lateralized in the motor cortex in accordance with the injured limb.
- To determine associations between pain-like behavior and estrogen/progesterone signaling, we will analyze correlations between paw withdrawal threshold and protein expression.

Alterations in Estrogen Signaling



Western blot analysis revealed that alcohol did not affect (A) estrogen receptor phosphorylation at Serine 118, (B) expression of total estrogen receptors, or (C) expression of GPER. (n=4-6 per group).

Research supported by grant # 1659752 through the National Science Foundation (NSF), Research Experiences for Undergraduates (REU) Program